

# Ultraviolet Coronagraph Spectroscopy: A Key Capability for Understanding the Physics of Solar Wind Acceleration

S. R. Cranmer,<sup>1</sup> J. L. Kohl,<sup>1</sup> D. Alexander,<sup>2</sup> A. Bhattacharjee,<sup>3</sup> B. A. Breech,<sup>4</sup> N. S. Brickhouse,<sup>1</sup> B. D. G. Chandran,<sup>3</sup> A. K. Dupree,<sup>1</sup> R. Esser,<sup>5</sup> S. P. Gary,<sup>6</sup> J. V. Hollweg,<sup>3</sup> P. A. Isenberg,<sup>3</sup> S. W. Kahler,<sup>7</sup> Y.-K. Ko,<sup>8</sup> J. M. Laming,<sup>8</sup> E. Landi,<sup>9</sup> W. H. Matthaeus,<sup>10</sup> N. A. Murphy,<sup>1</sup> S. Oughton,<sup>11</sup> J. C. Raymond,<sup>1</sup> D. B. Reisenfeld,<sup>12</sup> S. T. Suess,<sup>13</sup> A. A. van Ballegoijen,<sup>1</sup> and B. E. Wood<sup>8</sup>

<sup>1</sup>Harvard-Smithsonian CfA, <sup>2</sup>Rice University, <sup>3</sup>U. New Hampshire, <sup>4</sup>U.S. Army Research Laboratory, <sup>5</sup>U. Tromsø, Norway, <sup>6</sup>Los Alamos National Laboratory, <sup>7</sup>Air Force Research Laboratory, <sup>8</sup>Naval Research Laboratory, <sup>9</sup>U. Michigan, <sup>10</sup>Bartol Research Institute, U. Delaware, <sup>11</sup>U. Waikato, New Zealand, <sup>12</sup>U. Montana, <sup>13</sup>National Space Science & Technology Center

## Abstract

Understanding the physical processes responsible for accelerating the solar wind requires detailed measurements of the collisionless plasma in the extended solar corona. Some key clues about these processes have come from instruments that combine the power of an ultraviolet (UV) spectrometer with an occulted telescope. This combination enables measurements of ion emission lines far from the bright solar disk, where most of the solar wind acceleration occurs. Although the UVCS instrument on *SOHO* made several key discoveries, many questions remain unanswered because its capabilities were limited. This white paper summarizes these past achievements and also describes what can be accomplished with next-generation instrumentation of this kind.

## 1. Background and Motivation

The hot, ionized outer atmosphere of the Sun is a unique testbed for the study of magnetohydrodynamics (MHD) and plasma physics, with ranges of parameters that are inaccessible on Earth. Although considerable progress has been made during the last few decades, we still do not know the basic physical processes responsible for heating the million-degree solar corona and accelerating the solar wind. Identifying these processes is important not only for understanding the origins and impacts of space weather (e.g., Schwenn 2006; Eastwood 2008), but also for establishing a baseline of knowledge about a well-resolved star that is directly relevant to other astrophysical systems.

In order to construct and test theoretical models, a wide range of measurements of relevant plasma parameters must be available. In the low-density, open-field regions that reach into interplanetary space, more parameters need to be measured (in comparison to collision-dominated regions) because the plasma becomes **collisionless**. In other words, individual particle species—e.g., protons, electrons, helium, and minor ions—can exhibit different properties from one another. Such differences in particle velocity distributions are valuable probes of “microscopic” processes of heating and acceleration. In interplanetary space, such kinetic properties have been measured for decades by *in situ* particle instruments (e.g., Marsch 1999, 2006; Kasper et al. 2008). However, measurements in the near-Sun regions that are being actively heated and accelerated have been more limited in scope.

Remote-sensing measurements of plasma properties in the so-called “extended solar corona” (above about  $1.5 R_{\odot}$  measured from Sun-center) are difficult to make because the photon emission at large heights is fainter by many orders of magnitude than the emission from the solar disk. Standard telescopes, that do not explicitly block out the solar disk, typically contain enough scattered light from the disk to totally mask the faint off-limb emission. Because the corona is highly ionized, the dominant spectral features are at wavelengths accessible only from space. For these reasons, a series of Ultraviolet Coronagraph Spectrometer (UVCS) instruments have been built and flown on rockets, on a Shuttle-deployed *Spartan* payload, and as an instrument on the *Solar and Heliospheric Observatory (SOHO)* spacecraft; see, e.g., Kohl et al. (1978,

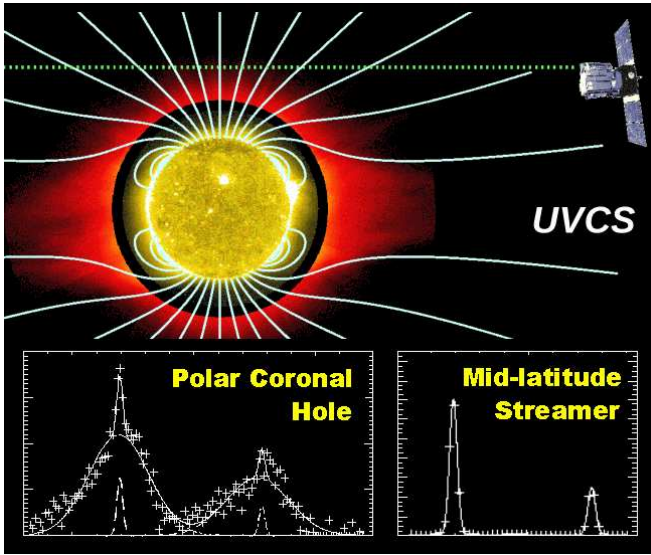


**Figure 1:** Combined *SOHO* image of the solar corona from 17 August 1996, showing the solar disk in Fe XII 195 Å intensity from EIT (yellow inner image) and the extended corona in O VI 1032 Å intensity from UVCS (red outer image). A typical UVCS observational line of sight is shown in green. Axisymmetric field lines are from the solar-minimum model of Banaszkiewicz et al. (1998), and O VI emission line profiles (bottom) are from various UVCS observations at  $r > 2R_{\odot}$  in 1996–1997 (Kohl et al. 1997).

1994, 1995, 1997, 2006). In these instruments, the coronagraphic blocking of bright light from the solar disk is done efficiently with a pair of occulters: one external to the telescope and one internal. Figure 1 illustrates UVCS/*SOHO* observations of the extended corona.

By measuring off-limb emission lines formed both by collisional excitation and by the scattering of solar-disk photons, UV spectroscopy provides a multi-faceted characterization of the kinetic properties of atoms, ions, and free electrons (e.g., Withbroe et al. 1982; Kohl et al. 2006). The Doppler-broadened shapes of emission lines are direct probes of line-of-sight (LOS) particle velocity distributions (i.e., essentially providing  $T_{\perp}$  when the off-limb magnetic field is  $\sim$ radial). Red/blue Doppler shifts reveal bulk flows along the LOS. Integrated intensities of resonantly scattered lines can be used to constrain the solar wind velocity and other details about the velocity distribution in the radial direction (e.g.,  $u_{\parallel}$  and  $T_{\parallel}$ ); this is the so-called “Doppler dimming/pumping” diagnostic (e.g., Noci et al. 1987). Intensities of collisionally dominated lines—especially when combined into an emission measure distribution—can constrain electron temperatures, densities, and elemental abundances in coronal plasma. Even departures from Maxwellian and bi-Maxwellian velocity distributions are detectable with spectroscopic measurements having sufficient sensitivity and spectral resolution.

In the **fast solar wind**, UVCS/*SOHO* measured outflow speeds that become supersonic much closer to the Sun than previously believed. In coronal holes, heavy ions (e.g.,  $O^{+5}$ ) were found to flow faster than the protons, to be heated hundreds of times more strongly than protons and electrons, and to have anisotropic temperatures with  $T_{\perp} > T_{\parallel}$  (Kohl et al. 1997, 1998, 1999; Cranmer et al. 1999b). Specifically, the anisotropic and super-heated oxygen velocity distributions (with  $T_{\perp} > 10^8$  K) have guided theorists to discard some candidate physical processes and further investigate others. Hollweg & Isenberg (2002) stated in a review paper that “We have seen that the information provided by UVCS has been pivotal in defining how research has proceeded during the past few years.”<sup>1</sup>

Figure 2 gives more information about how the temperatures of protons, electrons, and an example minor ion species ( $O^{+5}$  in the corona,  $O^{+6}$  *in situ*) differ from one another in the high-speed solar wind. Although the measured kinetic temperatures for protons are of order 2–3.5 MK, these are combinations of random thermal motions and “nonthermal” broadening due to Alfvén waves or other unresolved line-

<sup>1</sup>More recently, these results were highlighted in Chapter 3 of the 2010 report of the APS-sponsored Workshop on Opportunities in Plasma Astrophysics (WOPA); see <http://www.pppl.gov/conferences/2010/WOPA/>

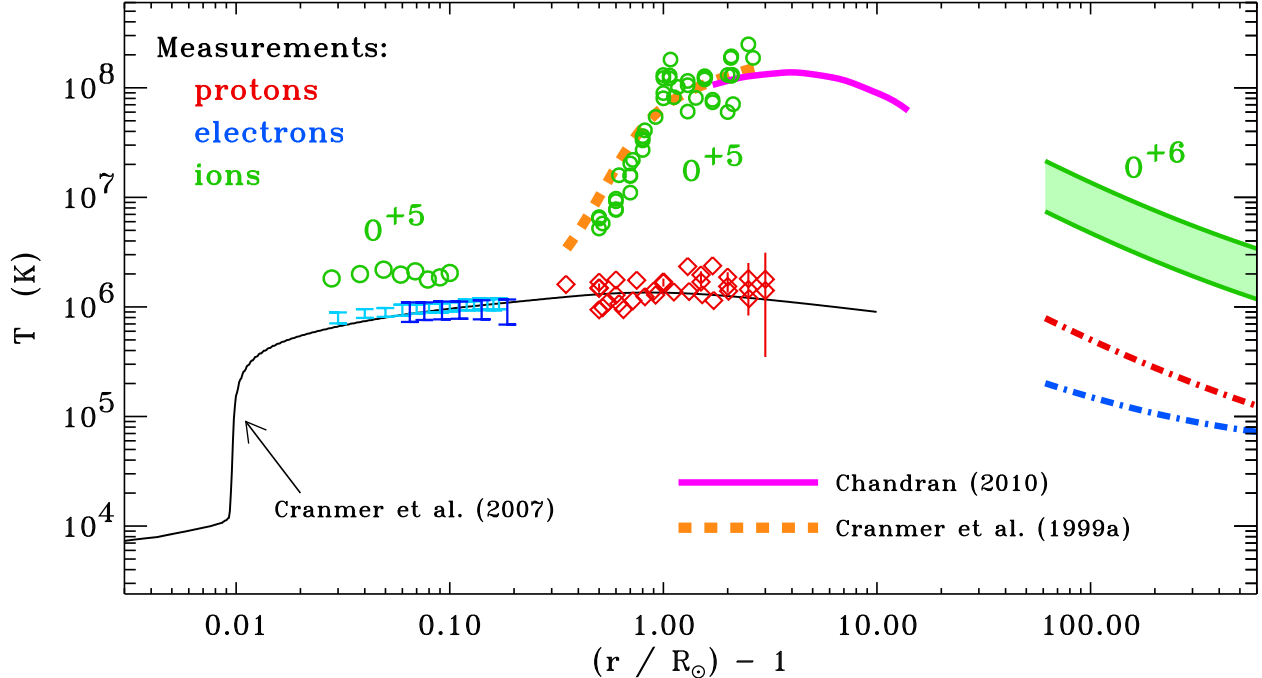


**Figure 2:** Radial dependence of temperatures in polar coronal holes and fast wind streams. Mean plasma temperature from a turbulence-driven coronal heating model (solid black curve; Cranmer et al. 2007).  $T_e$  from off-limb SUMER measurements made by Wilhelm (2006) (dark blue bars) and Landi (2008) (light blue bars).  $T_p$  from UVCS data assembled by Cranmer (2004) (red symbols). Perpendicular  $O^{+5}$  ion temperatures (green circles) from Landi & Cranmer (2009) ( $r < 1.1R_\odot$ ) and Cranmer et al. (2008) ( $r > 1.5R_\odot$ ). *In situ* values of  $T_p$  and  $T_e$  (red and blue dot-dashed curves) at  $r > 60R_\odot$  are from Cranmer et al. (2009), and the *in situ* range for  $O^{+6}$  (light green region) is inferred from, e.g., Collier et al. (1996). Ion heating theories assuming high- $k_\perp$  waves (magenta solid curve) and high- $k_\parallel$  waves (orange dashed curve) both appear to succeed in modeling the  $O^{+5}$  data.

of-sight motions. In Figure 2 we attempted to remove the contribution of waves to show the true proton temperatures. The resulting  $T_p$  does not show as clear a signal of preferential heating (relative to  $T_e$ ) as one would have seen from just the kinetic temperature. Although one can still marginally see that  $T_p > T_e$ , the existing measurements of  $T_p$  and  $T_e$  do not overlap with one another in radius. Improved measurements are needed in order to better constrain the proton and electron heating rates in the corona. The green points in Figure 2 indicate the key measurements of preferential  $O^{+5}$  heating in polar coronal holes. The magenta and orange curves show a subset of the many theoretical models that have been constructed to explain these data.

At solar minimum, UVCS/SOHO found that the **slow solar wind** flows mostly along the outer edges of bright streamers, near locations with measured abundance patterns matching those of the *in situ* slow wind (Raymond et al. 1997; Strachan et al. 2002; Abbo et al. 2010). The closed-field “core” regions of streamers, however, exhibit heavy element abundances only 3% to 30% of those seen at 1 AU, indicating gravitational settling (e.g., Raymond 1999; Vásquez & Raymond 2005) or complex flux-tube geometries (Noci et al. 1997). UVCS observed the transition from a high-density collision-dominated plasma at low heights in streamers to a low-density collisionless plasma at large heights, the latter exhibiting high ion temperatures and anisotropies that suggest similar physics as in the fast wind (Frazin et al. 2003). UVCS has also been used to measure plasma properties of coronal mass ejections (CMEs) and put useful constraints on their reconnection rates, 3D flow velocities, energy budgets, magnetic helicities, and shock compression ratios (see, e.g., Raymond 2002; Kohl et al. 2006).

## 2. Next-Generation Capabilities Are Needed

Despite the advances outlined above, the diagnostic capabilities of UVCS were limited to what was foreseen before the *SOHO* era (when only H I Ly $\alpha$  had been observed). Thus, we are still severely limited in our ability to answer the fundamental questions by our lack of knowledge of the plasma properties in the solar wind's acceleration region. The following enhancements in measurement capability are needed to be able to conclusively identify and characterize the processes that energize the solar wind.

- a. The key UVCS discovery of preferential ion heating and anisotropic ion velocity distributions near the Sun was essentially limited to just one ion (O<sup>+5</sup>). If the kinetic properties of **additional minor ions** were to be measured in the extended corona (i.e., a wider sampling of charge/mass combinations) we could much better determine the nature of the dominant collisionless heating process. Specifically, these measurements would provide an improved empirical description of kinetic waves and turbulence in the corona, with which we could conclusively identify the type of fluctuations (such as ion cyclotron waves, kinetic Alfvén waves, or other nonlinear turbulent modes) as well as their means of dissipation (Hollweg & Isenberg 2002; Cranmer 2002, 2009). Sampling as broad a range as possible in the ion charge-to-mass ratio ( $Z/A$ ) provides a sensitive probe of the heating; e.g., S<sup>+5</sup> (933 Å,  $Z/A = 0.16$ ), Ca<sup>+9</sup> (557 Å,  $Z/A = 0.22$ ), Si<sup>+8</sup> (296 Å,  $Z/A = 0.28$ ), O<sup>+5</sup> (1032 Å,  $Z/A = 0.31$ ), Mg<sup>+9</sup> (610 Å,  $Z/A = 0.37$ ), and Si<sup>+11</sup> (499 Å,  $Z/A = 0.39$ ). With these ions, the two models shown in Figure 2 (which use either high- $k_{\perp}$  or high- $k_{\parallel}$  waves) would be clearly distinguished from one another; see also Leamon et al. (2000). Our confidence in the uniqueness of a successful model increases as the number of ions observed increases.
- b. UVCS provided new constraints on the heating of minor ions, but not so much on the heating of the primary proton–electron plasma. Observationally, the biggest missing piece is the **electron temperature** above  $\sim 1.5 R_{\odot}$ . Direct measurements of  $T_e$  from, e.g., the broad Thomson-scattered component of H I Ly $\alpha$ , would allow us to determine the bulk-plasma heating rate in different solar wind regions, as well as the partitioning of energy between protons and electrons. This partitioning is a key diagnostic of turbulence models (e.g., Matthaeus et al. 2003; Howes 2010) as well as a driver of the stability of helmet streamers (e.g., Endeve et al. 2004). The downward conduction of electron thermal energy—from the corona to the transition region—sets the base pressure and thus the mass flux of the solar wind (Withbroe 1988; Lie-Svendsen et al. 2002), thus making measurements of  $T_e(r)$  especially important. Improved observations of proton temperatures are also important, since the measured rates of proton heating can be compared directly with the energy available to protons in ion cyclotron waves (as constrained by future measurements of additional minor ions; see item [a] above) to reveal the relative importance of resonant wave heating to the primary plasma.
- c. In addition to protons and electrons, **helium** also plays a major role in the “primary” plasma of the solar wind. Helium may regulate the wind's mass flux (Hansteen et al. 1994) and set a lower limit on its outflow speed (Kasper et al. 2007). Preferential heating of alpha particles may even dominate the coronal heating close to the Sun and control how much heat is received by the protons (Liewer et al. 2001; Li 2003). Observations of the He II 304 Å and He I 584 Å lines can be used to measure the coronal helium abundance, departures from ionization equilibrium, and the amount of preferential alpha-particle heating.
- d. Space-based observations by *Hinode* and *SDO*, as well as ground-based eclipse observations, have highlighted the importance of **greater spatial and temporal resolution** to the direct identification of MHD waves with periods between about 0.1 and 10 minutes (De Pontieu et al. 2007; Pasachoff et al. 2002; Singh et al. 2009). The predicted amplitudes of most MHD waves grow significantly as they propagate up to the extended corona, thus making a UVCS-type instrument with greater sensitivity and resolution ideal for detecting both compressive waves (via intensity oscillations) and Alfvén waves (via Doppler shifts). Measuring the frequency and wavenumber dependence of these waves would open new windows on our understanding of coronal turbulence (e.g., Matthaeus et al. 1999). Greater spatial and temporal resolution also allows improved characterization of small-scale inhomogeneities between neighboring

flux tubes in coronal holes and streamers. Precise measurements of cross-field density gradients can put firm constraints on models of coronal heating via drift instabilities (e.g., Mecheri & Marsch 2008) and MHD discontinuities in the solar wind (Feldman et al. 1997; Borovsky 2008).

- e. Recent analysis of *in situ* data shows that the combined **elemental abundances and charge states** of solar wind ions can be used to effectively probe the origin of heliospheric wind streams in closed or open flux tubes (Zurbuchen 2007). There have been some isolated comparisons of ion composition between UVCS and *in situ* measurements (e.g., Ko et al. 2006), but higher resolution and greater sensitivity to more ions is needed to produce corona-heliosphere “mappings” of abundances and charge states that are detailed enough to test models of coronal gravitational settling and ion drag (Lenz 2004; Li et al. 2006) and the first ionization potential (FIP) effect (e.g., Laming 2004, 2009). It is also important to measure a broader range of low-FIP and high-FIP ions in order to better map out the way the solar atmosphere becomes fractionated.
- f. Measuring **non-Maxwellian velocity distributions** of electrons and positive ions would provide even more stringent tests of specific models of MHD turbulence, cyclotron resonance, and velocity filtration. An instrument with greater sensitivity than UVCS/*SOHO* could detect subtle departures from Gaussian line shapes that signal the presence of specific non-Maxwellian distributions (e.g., Cranmer 1998, 2001).

New capabilities such as these would be enabled by greater photon sensitivity, an expanded wavelength range, and the use of measurements that heretofore have been utilized only in a testing capacity (e.g., Thomson-scattered H I Ly $\alpha$  to obtain  $T_e$ ). These would allow the relative contributions of different physical processes to the heating and acceleration of all solar wind plasma components to be determined directly.

### 3. Synergy with Other Instrumentation and Missions

UV coronagraph spectroscopy has been a key asset to a large number of multi-instrument and multi-mission observation campaigns (e.g., Galvin & Kohl 1999). For example, coordinated observations taken at times when *SOHO* and *Ulysses* could track the same plasma parcels from the Sun to the outer heliosphere led to new methods of mapping field lines over long distances in the solar wind (Suess et al. 2000; Poletto et al. 2002). Next-generation UVCS-type measurements would also provide key context for the regions of the inner heliosphere that *Solar Probe Plus (SPP)* and *Solar Orbiter* will fly through, and they would provide direct measurements of coronal regions inaccessible even to *SPP* (i.e.,  $r < 9 R_\odot$ ).

Measurements from other instruments also can enhance the ability of UV coronagraph spectroscopy to determine coronal plasma parameters. Although UV emission lines can be used to measure the coronal electron density (e.g., Noci et al. 1997; Antonucci et al. 2004), the most straightforward method to obtain  $n_e$  has been the analysis of polarized brightness measured by a white-light coronagraph. The combination of a UVCS-type instrument and a white-light imaging coronagraph provides useful diagnostics that extend beyond what is possible with either instrument in isolation.

There are several possible mission concepts for next-generation UV coronagraph spectrometers. Sub-orbital rockets are useful for demonstrating the capabilities of this kind of instrument, as well as being able to obtain useful scientific results (see § 4.1 of Kohl et al. 2006). Studies have also shown that a standard Low-Earth orbit (350–600 km altitude at 28° latitude) can provide adequate observation time, low UV optical depth from the Earth’s atmosphere, and negligible contamination to enable the full range of required UV coronagraph spectroscopy. A polar, Sun-synchronous orbit would of course be an improvement over a low-latitude orbit because of the lack of diurnal solar occultation by the Earth. Another possibility is to position the spacecraft at the **Earth-Sun L5 point** (see also Vourlidas et al. 2010) which eliminates issues of atmospheric absorption and orbital night. This location also positions the prime off-limb field of view (i.e., the “plane of the sky”) close to the Earth-Sun line, so that geoeffective solar wind streams and CMEs can be measured directly.

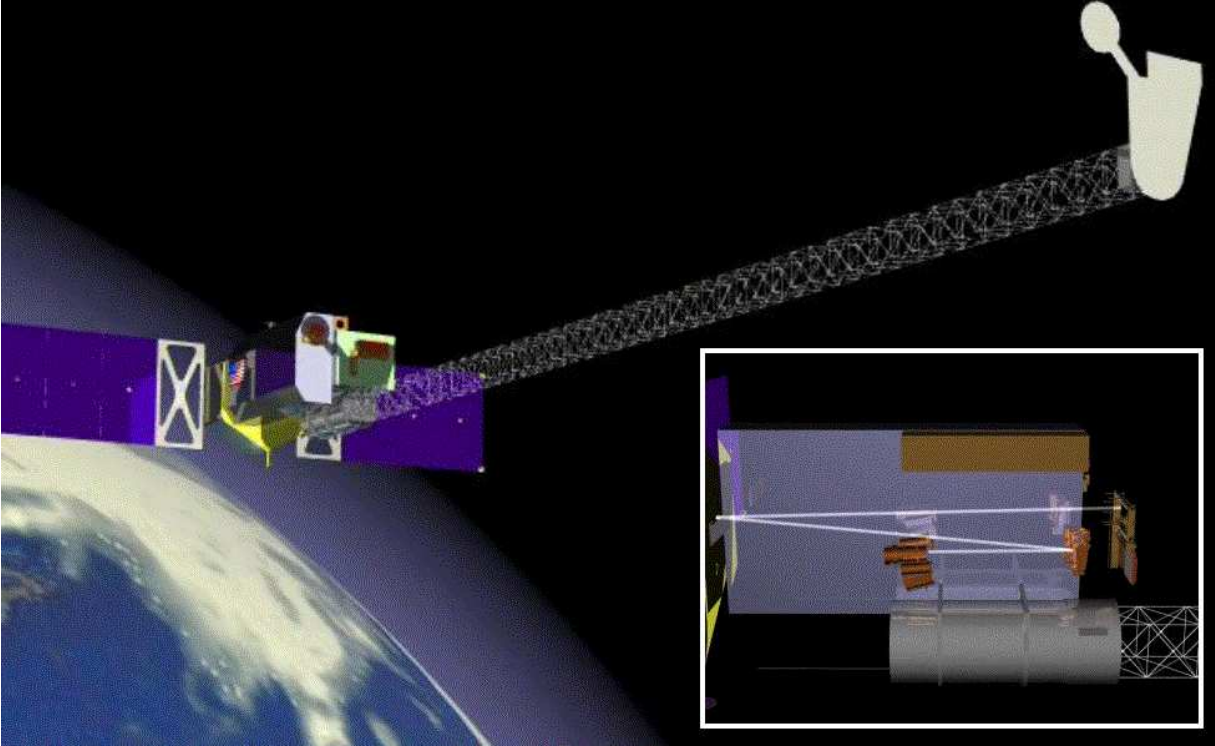


**Figure 3:** Spacecraft concept for a large-aperture UV coronagraph with an external occulter at the end of a 13 m boom. The inset shows a diagram of an advanced LAUVCS instrument (see Kohl et al. 2006).

#### 4. Instrumentation and Costs

The UV spectroscopic observations required to produce detailed empirical descriptions of solar wind source regions can be accomplished with a large-aperture ultraviolet coronagraph spectrometer (LAUVCS). The large aperture is needed to provide the sensitivity to observe relatively weak spectral lines with the required range of charge-to-mass ratios. The large aperture can be realized with a remote external occulter supported by a deployable mast (see Figure 3). Such an instrument would accommodate a much larger telescope area than UVCS/SOHO that is both shielded from direct solar disk rays and also has an unobstructed view of the coronal heights of interest. When equipped with state-of-the-art reflection coatings, high ruling efficiency diffraction gratings, and array detectors, such an instrument exceeds the sensitivity and stray light suppression needed to make all required coronal observations in both streamers and coronal holes up to at least  $5 R_{\odot}$  and often higher. It is also possible to achieve the large aperture with an internally occulted coronagraph where the solar-disk radiation impinges directly on the telescope primary. The sensitivity is just as good as that of the externally occulted instrument, but the stray light characteristics only allow observations up to  $\sim 2R_{\odot}$  in coronal holes and  $\sim 3R_{\odot}$  in streamers. Compared to UVCS, either instrument would make a tremendous step forward in describing solar wind source regions and identifying the physical processes that heat and accelerate the solar wind (and CMEs<sup>2</sup>).

Both externally occulted and internally occulted LAUVCS type instruments can be built with existing technology. Deployable masts to support the remote external occulter, such as the one baselined for the *NuSTAR* mission, are commercially available. There is also “in space” performance data that demonstrates the ATK ADAM mast exceeds the specifications required for the externally occulted LAUVCS. Intensified

---

<sup>2</sup>The ability of next-generation UV coronagraph spectroscopy to answer fundamental questions about how CMEs and solar energetic particles (SEPs) are produced will be described in a separate white paper.

CCD (ICCD) detectors similar to those used on *XMM* and *Swift* can be used for a LAUVCS, and they are capable of meeting all requirements for the solar wind science while maintaining the full instrument sensitivity. The KBr-coated microchannel plates that are needed to meet the UV sensitivity requirements are also available commercially, and they can be incorporated into an ICCD with an acceptable air exposure. To achieve the LAUVCS science objectives for CMEs—without the need to attenuate the associated high light levels—it is highly desirable to use an intensified active pixel sensor (IAPS), which is the next step beyond the ICCD. A laboratory model of such a device exists at the Mullard Space Science Laboratory (MSSL), and it has been clocked at 66 MHz to achieve the desired maximum detection rate of 32 Hz per pixel with less than a 10% dead time loss.

Both the solar wind and the baseline CME science objectives can be achieved with an ICCD detector similar to those flown on *XMM* and *Swift*. The advanced technology IAPS detectors currently being developed at MSSL are showing great promise, and they could provide a dynamic range and maximum count rate capability that would accommodate the bright CME emissions without the need for attenuators.

The cost (in FY 2011 dollars) of an externally occulted LAUVCS for a Class C mission with limited redundancy, including design, development, calibration, environmental testing, and support for integration, is approximately \$45M including the cost of the deployable mast. The cost of the internally occulted instrument would be about \$15M less. These estimated costs do not include any reserve/contingency or margin except for costed schedule reserve, and they do not include any Phase E mission operation and data analysis costs.

## References

- Abbo, L., et al. 2010, *Adv. Sp. Res.*, 46, 1400  
 Antonucci, E., et al. 2004, *A&A*, 416, 749  
 Banaszekiewicz, M., et al. *A&A*, 337, 940  
 Borovsky, J. E. 2008, *JGR*, 113, A08110  
 Chandran, B. D. G. 2010, *ApJ*, 720, 548  
 Collier, M. R., et al. 1996, *GRL*, 23, 1191  
 Cranmer, S. R. 1998, *ApJ*, 508, 925  
 Cranmer, S. R. 2001, *JGR*, 106, 24937  
 Cranmer, S. R. 2002, *Proc. SOHO-11*, 361, astro-ph/0209301  
 Cranmer, S. R. 2004, *Proc. SOHO-15*, 154, astro-ph/0409724  
 Cranmer, S. R. 2009, *Living Rev. Sol. Phys.*, 6, 3  
 Cranmer, S. R., et al. 1999a, *ApJ*, 518, 937  
 Cranmer, S. R., et al. 1999b, *ApJ*, 511, 481  
 Cranmer, S. R., et al. 2007, *ApJS*, 171, 520  
 Cranmer, S. R., et al. 2008, *ApJ*, 678, 1480  
 Cranmer, S. R., et al. 2009, *ApJ*, 702, 1604  
 De Pontieu, B., et al. 2007, *Science*, 318, 1574  
 Eastwood, J. P. 2008, *Phil. Trans. Roy. Soc. A*, 366, 4489  
 Endeve, E., et al. 2004, *ApJ*, 603, 307  
 Feldman, W. C., et al. 1997, *JGR*, 102, 26905  
 Frazin, R. A., et al. 2003, *ApJ*, 597, 1145  
 Galvin, A. B., & Kohl, J. L. 1999, *JGR*, 104, 9673  
 Hansteen, V. H., et al. 1994, *ApJ*, 428, 843  
 Hollweg, J. V., & Isenberg, P. A. 2002, *JGR*, 107 (A7), 1147  
 Howes, G. G. 2010, *MNRAS*, in press, arXiv:1009.4212  
 Kasper, J. C., et al. 2007, *ApJ*, 660, 901  
 Kasper, J. C., et al. 2008, *PRL*, 101, 261103  
 Ko, Y.-K., et al. 2006, *ApJ*, 646, 1275  
 Kohl, J. L., et al. 1978, in *New Instrumentation for Space Astronomy* (Oxford: Pergamon), 91  
 Kohl, J. L., et al. 1994, *Space Sci. Rev.*, 70, 253  
 Kohl, J. L., et al. 1995, *Solar Phys.*, 162, 313  
 Kohl, J. L., et al. 1997, *Solar Phys.*, 175, 613  
 Kohl, J. L., et al. 1998, *ApJ*, 501, L127  
 Kohl, J. L., et al. 1999, *ApJ*, 510, L59  
 Kohl, J. L., et al. 2006, *A&A Review*, 13, 31  
 Laming, J. M. 2004, *ApJ*, 614, 1063  
 Laming, J. M. 2009, *ApJ*, 695, 954  
 Laming, J. M., & Lepri, S. T. 2007, *ApJ*, 660, 1642  
 Landi, E. 2008, *ApJ*, 685, 1270  
 Landi, E., & Cranmer, S. R. 2009, *ApJ*, 691, 794  
 Leamon, R. J., et al. 2000, *ApJ*, 537, 1054  
 Lenz, D. D. 2004, *ApJ*, 604, 433  
 Li, B., et al. 2006, *JGR*, 111, A08106  
 Li, X. 2003, *A&A*, 406, 345  
 Lie-Svendsen, Ø., et al. 2002, *ApJ*, 566, 562  
 Liewer, P., et al. 2001, *JGR*, 106, 29261  
 Marsch, E. 1999, *Space Sci. Rev.*, 87, 1  
 Marsch, E. 2006, *Liv. Rev. Sol. Phys.*, 3, 1  
 Matthaeus, W. H., et al. 1999, *ApJ*, 523, L93  
 Matthaeus, W. H., et al. 2003, *Nonlin. Proc. Geophys.*, 10, 93  
 Mecheri, R., & Marsch, E. 2008, *A&A*, 481, 853  
 Noci, G., et al. 1987, *ApJ*, 315, 706  
 Noci, G., et al. 1997, *Proc. SOHO-5*, ESA SP-404, 75  
 Pasachoff, J. M., et al. 2002, *Solar Phys.*, 207, 241  
 Poletto, G., et al. 2002, *JGR*, 107, 1300  
 Raymond, J. C. 1999, *Space Sci. Rev.*, 87, 55  
 Raymond, J. C. 2002, *Proc. SOHO-11*, ESA SP-508, 421  
 Raymond, J. C., et al. 1997, *Solar Phys.*, 175, 645  
 Schwenn, R. 2006, *Liv. Rev. Sol. Phys.*, 3, 2  
 Singh, J., et al. 2009, *Solar Phys.*, 260, 125  
 Strachan, L., et al. 2002, *ApJ*, 571, 1008  
 Suess, S. T., et al. 2002, *JGR*, 105, 25033  
 Vásquez, A. M., & Raymond, J. C. 2005, *ApJ*, 619, 1132  
 Vourlidas, A., et al. 2010, *NRC Decadal Survey White Paper*  
 Wilhelm, K. 2006, *A&A*, 455, 697  
 Withbroe, G. L. 1988, *ApJ*, 325, 442  
 Withbroe, G. L., et al. 1982, *Space Sci. Rev.*, 33, 17  
 Zurbuchen, T. H. 2007, *Ann. Rev. Astron. Astrophys.*, 45, 297